Technical Paper
J. Astron. Space Sci. 35(3), 195-200 (2018)
https://doi.org/10.5140/JASS.2018.35.3.195

JASS Journal of Astronomy and Space Sciences

Conceptual Design of a Solid State Telescope for Small scale magNetospheric Ionospheric Plasma Experiments

Jongdae Sohn[1†], Jaejin Lee[1], Gyeongbok Jo[1], Jongkil Lee[1], Junga Hwang[1], Jaeheung Park[1], Young-Sil Kwak[1], Won-Kee Park[1], Uk-Won Nam[1], Kyunghwan Dokgo[2]

[1]Korea Astronomy and Space Science Institute, Daejeon 34055, Korea
[2]Southwest Research Institute, San Antonio, TX 73238, USA

The present paper describes the design of a Solid State Telescope (SST) on board the Korea Astronomy and Space Science Institute satellite-1 (KASISat-1) consisting of four [TBD] nanosatellites. The SST will measure these radiation belt electrons from a low-Earth polar orbit satellite to study mechanisms related to the spatial resolution of electron precipitation, such as electron microbursts, and those related to the measurement of energy dispersion with a high temporal resolution in the sub-auroral regions. We performed a simulation to determine the sensor design of the SST using GEometry ANd Tracking 4 (GEANT4) simulations and the Bethe formula. The simulation was performed in the range of 100 ~ 400 keV considering that the electron, which is to be detected in the space environment. The SST is based on a silicon barrier detector and consists of two telescopes mounted on a satellite to observe the electrons moving along the geomagnetic field (pitch angle 0°) and the quasi-trapped electrons (pitch angle 90°) during observations. We determined the telescope design of the SST in view of previous measurements and the geometrical factor in the cylindrical geometry of Sullivan (1971). With a high spectral resolution of 16 channels over the 100 keV ~ 400 keV energy range, together with the pitch angle information, the designed SST will answer questions regarding the occurrence of microbursts and the interaction with energetic particles. The KASISat-1 is expected to be launched in the latter half of 2020.

Keywords: solid state telescope, electron, microburst, precipitation

1. INTRODUCTION

Solar activity driven by the solar magnetic field takes many forms such as solar flares, coronal mass ejections (CMEs), high-speed solar wind, and solar energetic particles. This solar activity associated with space weather has lasting effects on ground-based systems, satellites, and the Earth's magnetosphere. It also causes solar limb darkening, solar wind density depletions in the solar cycle, changes in the solar wind density on the Martian bow shock, and alterations in the local distribution of lunar hydroxyl influenced by the solar insolation effect on the space environment in the solar system (Kim et al. 2011; Moon et al. 2017; Park et al. 2017; Kim et al. 2018). We can use data from neutron monitors recently installed in Jang Bogo station (Jung et al. 2016) on the ground to study the space environment. We have access to data from the High Energy Particle Detector (HEPD) (Sohn et al. 2012; Jo et al. 2014; Sohn et al. 2018) of Instruments for the study of Stable/Storm-time Space (ISSS) (Choi et al. 2014) onboard the Next Generation Small Satellite-1 (NEXTSat-1) (Shin et al. 2014a, b), which will be launched this year, to understand the plasma structures in the near-Earth space environment.

The Korea Astronomy and Space Science Institute satellite-1 (KASISat-1), consisting of four [TBD] nanosatellites, is scheduled for launch in the second half of 2020 for Small scale magNetospheric Ionospheric Plasma Experiments (SNIPE) to elucidate the properties of microscale (100

This is an Open Access article distributed under the terms of the Creative Commons Attribution Non-Commercial License (https://creativecommons.org/licenses/by-nc/3.0/) which permits unrestricted non-commercial use, distribution, and reproduction in any medium, provided the original work is properly cited.

Received 27 AUG 2018 **Revised** 4 SEP 2018 **Accepted** 5 SEP 2018
†**Corresponding Author**
Tel: +82-42-869-5906, E-mail: jdsohn@kasi.re.kr
ORCID: https://orcid.org/0000-0002-6572-622X

m–10 km) structures in the topside ionosphere (below the altitude of 1,000 km), particularly the fine-scale morphology of high-energy electron precipitation, cold plasma density/temperature, field-aligned currents, and electromagnetic waves. In order to work out the spatial and temporal variations of microscale plasma structures, the SNIPE mission consisting of four (TBD) nanosatellites (approximately 12 kg) will have a polar orbit at an altitude of 500–600 km (TBD). Two pairs of satellites will be deployed in orbit and the distances between each satellite will be in the range of 10 to 100 km, controlled by a formation flying algorithm. The SNIPE mission is equipped with scientific payloads which can measure the following geophysical parameters: the density/temperature of cold ionospheric electrons, energetic (100 keV ~ 1 MeV) electron flux, and magnetic field vectors. Among them, the Solid State Telescope (SST) will observe hundreds of keV of electron precipitations such as electron microbursts.

Electron microbursts are short duration (less than 1 sec) energetic electron precipitations into the Earth's atmosphere, mainly observed in the recovery phase of geomagnetic storms at L=4–8 and 06–18 local times (Parks 1978). They were first discovered by X-ray balloon-borne experiments in the early sixties (Anderson and Milton, 1964). Electron microbursts with an energy > 40 keV were observed by the INJUN-3 satellite launched in 1963, after which Imhof et al. (1992) and Nakamura et al. (2000) reported observations of impulsive electron precipitation with energies > 1 MeV using a spacecraft experiment and called them relativistic microbursts. Electron microbursts were observed by STSAT-1, launched in 2003, which decomposed the parallel and perpendicular components of the particle flux. The observation, performed in the recovery phase of the geomagnetic storm that occurred on November 10, 2004, shows a microburst train composed of fine structures with a time duration less than 1 sec for 30 sec (Lee et al. 2005). Through this experiment, it was confirmed that the perpendicular (quasi-trapped) microbursts have harder energy spectra than the parallel (precipitating) microbursts, and that the loss cone is not filled.

Considering that the time duration of a microburst is less than 1 sec, a microburst electron should be generated by fast pitch angle diffusion somewhere in the middle of the bounce motion, because the captured 100 keV electron requires approximately 1 sec to undergo a bounce motion in the north–south direction. Therefore, the time taken to reach a low-Earth orbit (approximately 600 km) is determined by the location of the wave-particle interaction and the velocity of the electrons. Therefore, an energy dispersion should be observed if the microburst is observed with a sufficient time resolution. However, there is no report of observations of such an energy dispersion.

In our experiment, we observed the energy dispersion of the electron microburst and investigated the interactions of the energetic electrons with the chorus wave. The observations by multiple low-orbit satellites are expected to answer the following scientific questions.

1. How does the small electron precipitation structure exist and what is the mechanism of this precipitation phenomenon?

2. How do electron microbursts interact with waves?

3. How large is the contribution of the radiation belt loss owing to the microburst precipitation?

This paper discusses the instrument design of the SST on board KASISat-1. The Conceptual Design of the SST is delineated in Sec. II. The Expected Results are described in Sec. III. Finally, The Discussion and Conclusion are presented in Sec. IV.

2. CONCEPTUAL DESIGN OF THE SST

2.1 Previous Measurements and SST Requirements

The electron flux measured by Science and Technology SATellite-1 (STSAT-1)-1 was below 104 $(cm^2 \text{ sec sr keV})^{-1}$ at 100 keV and below 103 $(cm^2 \text{ sec sr keV})^{-1}$ at 300 keV for the electron microbursts observed at solar maximum (Lee et al. 2005, 2006). Electron microbursts are observed at 50–70° during the storm recovery phase, mainly at dawn. This mission shall be launched in 2020. At that time, small storms may occur approximately two or three times a month. We will observe several microbursts with durations of less than 1 sec. The microbursts should partially fill the loss cone. Further, the flux will be observed differently depending on the pitch angle. In order to obtain approximate pitch angle information, two SSTs will be mounted: one in parallel to the Earth's magnetic field, and the other perpendicular. The SST observing the energetic electrons should be designed to have a fast sampling rate to enable observation of the microburst. The microburst will be observed in the fast mode in order to observe the energy dispersion of the microburst. The SST will measure energetic electrons with energies from ~ 100 keV to 400 keV at a low-Earth polar orbit to study the mechanisms related to the spatial resolution of electron precipitations, such as electron microbursts, and those related to the measurement of energy dispersion with a high temporal resolution in the sub-auroral regions.

2.2 Sensor Design

Energy spectra are obtained from the linear energy transfer (LET) delivered to the silicon detectors when the incident particles pass through the them. LET values are given by the Bethe Formula (Bethe & Ashkin 1953) and can be easily estimated by GEometry ANd Tracking 4 (GEANT4) simulations. Linear energy transfer (LET) is described as the amount of energy that an ionizing particle transfers to the material traversed per unit distance. If we ignore the energy loss due to the trajectory of the particles incident on the material, the Bethe Formula can be approximated to the LET shown in Eq. (1). According to the International Commission on Radiation Units and Measurements (ICRU) (1970), the LET of a particle incident on the material, as shown in Eq. (1), can be expressed as dE/dx, and dE is defined as the average energy transmitted to the material as the particle travels a distance of dx. Thus,

$$\Delta \mathbf{E} = \left(-\frac{dE}{dx}\right) \boldsymbol{t} \quad (1)$$

where t is the thickness of the material (thickness of the silicon sensor) and ($-dE/dx$) is the LET to the material (silicon sensor). This LET creates the electron-hole pairs in the material, which are then converted to an electrical signal by the bias voltage across the sensor. Since LET shows different patterns depending on the energy, material, and the incident particles, the energy loss was calculated by the Bethe Formula and estimated by using GEANT4 simulations. We performed the simulations to determine the sensor design of the SST using GEANT4 and the Bethe formula. Figs. 2 and 3 present the LET simulation results of the electron and the proton for the 0 – 500 keV range, after using GEANT4, for the SST structure described in Fig. 1 and Table 1. The simulation was performed in the range of 0 ~ 500 keV considering that the electron and the proton, which is to be detected in the space environment. A Nickel foil of 1 μm thickness was placed in front of the detector assembly to block low energy protons: the foil blocked protons with energies below ~ 200 keV. The LET values corresponding to the Solid State Detector (SSD) and Nickel are plotted in Figs. 2 and 3 for the electrons and protons that are incident on the detector. By using Nickel as a blocking material and adjusting the energy detection range based on these plots, we determined a total of 16 energy channels for the energy range of the SST. The detectors were the Fully Depleted Passivated Implanted Planar Silicon (PIPS) Detectors, FD series, with active areas of 50 mm2, which are commercially manufactured by CANBERRA. The SSD had a depletion depth of 500 μm. The SST was based on a silicon barrier

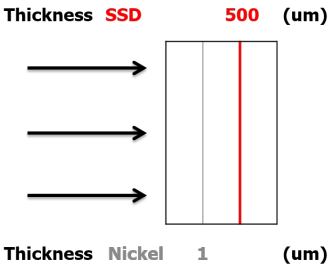

Fig. 1. Conceptual structure of Solid State Telescope (SST) [red: semiconductor detector [SSD], gray: Nickel [Ni], blocking material].

Table 1. Structure material and thickness of SST

Material	Thickness (mm)
Ni	0.001
SSD	0.5

SST: Solid State Telescope, Ni: Nickel,
SSD: Solid State Detector

detector and consisted of two telescopes that would be mounted on the satellite to observe the electrons moving along the geomagnetic field (pitch angle 0°) and the quasi-trapped electrons (pitch angle 90°) during observations.

2.3 Telescope Design

We determined the telescope design of the SST in view of previous measurements and the geometrical factor in the cylindrical geometry of Sullivan (1971). Assuming that the flux incident on the SST is a uniform flux, the counting rate (C) is given by following equation:

$$\mathbf{C} = \mathbf{G} \times \mathbf{I} \quad (2)$$

where I is the uniform flux and G is the geometrical factor.

The geometrical factor for the SST telescope was determined in view of previous measurements by STSAT-1. With this in mind, the telescope was designed with the geometrical factor G = 0.02 ($cm^2 \cdot sr$). If the geometric structure of the SST is assumed to be the symmetrical cylindrical geometry as shown in Fig. 2 of Sullivan (1971), the geometrical factor of the telescope is given by the following equation:

$$\mathbf{G} = \frac{1}{2}\pi^2 \left[R_1^2 + R_2^2 + H^2 - \left\{\left(R_1^2 + R_2^2 + H^2\right)^2 - 4 R_1^2 R_2^2\right\}^{1/2}\right] \quad (3)$$

where R_1 is the radius of the front aperture, R_2 is the radius of the rear aperture, and H is the distance between them. The geometrical structures as shown in Table 2 were calculated by a digital computer approximation simulation utilizing the Monte-Carlo method.

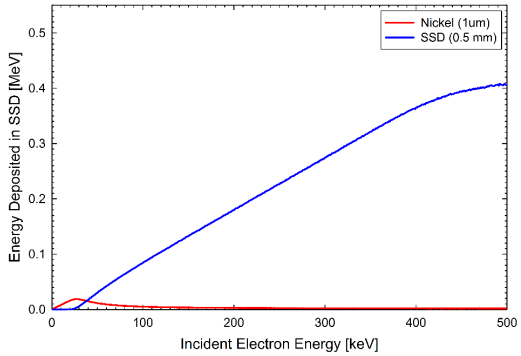

Fig. 2. Linear Energy Transfer (LET) simulation for the silicon detector SSD: Electron.

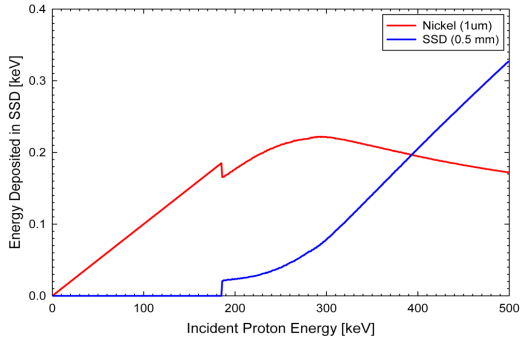

Fig. 3. Linear Energy Transfer (LET) simulation for the silicon detector SSD: Proton.

Table 2. Geometrical Structure and Field of View for the SST

Payload	Front Aperture Size (R1)	Rear Aperture Size (R2)	Distance (H)	G (cm^2·sr)	Field of View (°)
SST	0.9	0.17	3.2	0.020858	36.97729364

2.4 Electronics

As shown in Fig. 4, the analog signals generated by the electrons are converted into digital signals through signal processing systems. Then, they are finally delivered to the On-Board Computer (OBC) of the spacecraft via the Spacecraft Interface Board (SCIF B/D) for transmission to the ground station. We shall use an application-specific integrated circuit (ASIC) in our nano-satellite mission due to constraints for the size and power reduction of the payloads. Both the National Aeronautics and Space Administration (NASA) and the European Space Agency (ESA) are currently developing various chipsets for particle detection front-end and back-end electronics. Such low power, low noise, mixed analog-digital particle detector front-end (PDFE) custom chipsets shall be tested for our mission. The SST will have high temporal resolution and sampling rates of about 10~100 Hz (TBD).

3. EXPECTED RESULTS

The spatial scale of the electron microbursts was described by Crew et al. (2016); further, it is expected that each microburst has a different spatial size. Therefore, we will observe the spatial distribution of the microbursts via the experiment.

The results of the observation will be compared to the spatial scale of the chorus waves observed by large satellites operating in the equatorial high-altitude region. This could also explain the occurrence of the electron temperature anisotropy of the magnetic field. The spatial scales of the chorus waves obtained using the simulation code and the observations can be compared with each other. Moreover, the time-dependent scale of the electron microbursts can be calculated to obtain the number of electrons that penetrate the Earth's atmosphere via microburst phenomena.

The energy dispersion of the electron microbursts observed by the SST will help determine the locations of microburst occurrences. If the waves interact with electrons at a different latitude, the shape of the energy dispersion will be different.

As shown in Fig. 5, through the expected design structure of the SST for SNIPE, we will obtain the spatial scales and energy dispersion of the electron microbursts.

As shown in Fig. 6. The SST can have a sampling rate as high as 100 kHz by the SST analog board using the expected design structure.

4. DISCUSSION AND CONCLUSION

The SST for the SNIPE mission is focused on the spatial resolution of electron microbursts and the measurement of energy dispersion with a high temporal resolution. In order to observe electron microbursts, two SSTs capable of measuring electrons with energies in the range of 100 keV – 400 keV will be mounted on a satellite. One SST is intended for observing the electrons moving along the geomagnetic field (pitch angle 0°), the other SST is intended for measuring the quasi-trapped electrons (pitch angle 90°) during measurement. The direction of the Earth's magnetic field will be detected using a magnetometer mounted on the KASISat-1. To observe the spatial scale of the electron microbursts, the KASISat-1 consisting of four [TBD] nanosatellites will slowly separate the two satellites up to 100 km during the mission lifetime. It is expected that the statistical spatial scale of a microburst can be obtained. The spatial scale of the electron microbursts will indicate the spatial extent of chorus waves in the equatorial region and, eventually, the plasma irregularities. It is also known

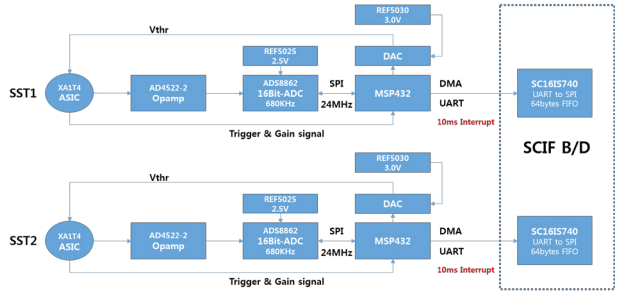

Fig. 4. SST system block diagram.

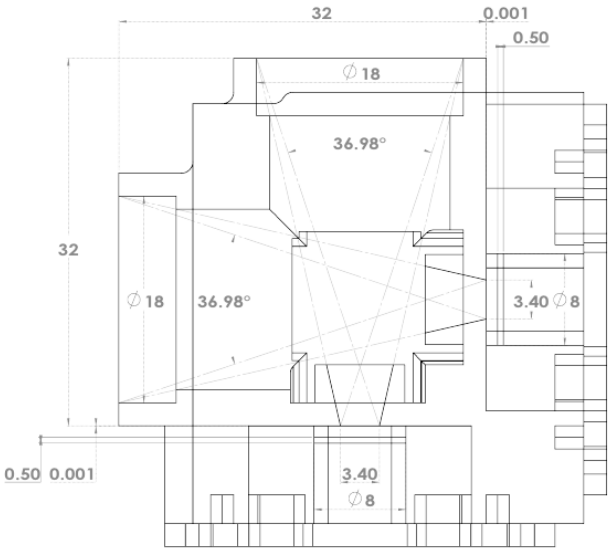

Fig. 5. The conceptual design of the Solid State Telescope [unit: mm].

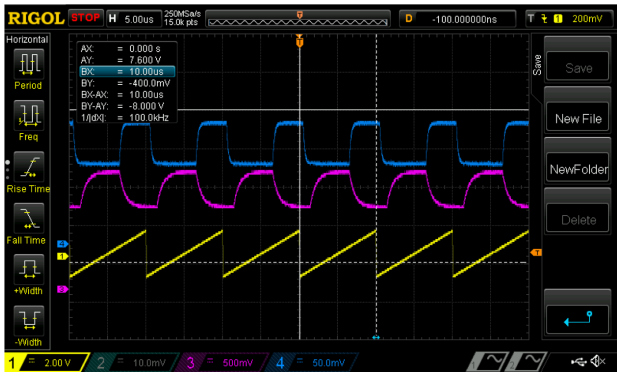

Fig. 6. Test result of sampling rate (100 kHz) by the SST analog board for SNIPE [Yellow line: test pulse Input, Blue line: trigger signal, Red line: output signal].

that, in the polar region, there are plasma structures with small spatial scales, although they have longer durations than electron microbursts. These structures are not easily distinguishable from the microbursts in a single satellite observation. However, multiple satellite observations, such as those of the SNIPE mission, will examine the existence of the small spatial scales of electron precipitation in the polar region. The measurement of the energy dispersions of microbursts will determine the location of the initiation of electron microbursts by wave-particle interactions. Thus, the SST for SNIPE will answer all questions regarding the occurrence of microbursts and the interactions with energetic particles

ACKNOWLEDGMENTS

This work was supported by basic research funding from the Korea Astronomy and Space Science Institute.

REFERENCES

Anderson KA, Milton DW, Balloon observations of X rays in the auroral zone: 3. high time resolution studies, J. Geohpys. Res. 69, 4457-4479 (1964). https://doi.org/10.1029/JZ069i021p04457

Bethe H, Ashkin J, Passage of radiations through matter, in Experimental Nuclear Physics, vol. 1, ed. Segrè E (Wiley, New York, 1953), 166-357.

Choi CR, Sohn JD, Lee JC, Seo YM, Kang SB, et al., Scientific Missions and Technologies of the ISSS on board the NEXTSat-1, J. Astron. Space Sci. 31, 73-81 (2014). https://doi.org/10.5140/JASS.2014.31.1.73

Crew AB, Spence HE, Blake JB, Klumpar DM, Larsen BA, et al., First multipoint in situ observations of electron microbursts: Initial results from the NSF FIREBIRD II mission, J. Geophys. Res. 121, 5272-5283 (2016). https://doi.org/10.1002/2016JA022485

ICRU, ICRU Report 16: Linear Energy Transfer (Oxford University Press, London, 1970), 2-5.

Imhof WL, Voss HD, Mobilia, J, Datlowe DW, Gaines EE, et al., Relativistic electron microbursts, J. Geophys. Res. 97, 13829-13837 (1992). https://doi.org/10.1029/92JA01138

Jo GB, Sohn JD, Choi CR, Yi Y, Min KW, et al., Development of high energy particle detector for the study of space radiation storm, J. Astron. Space Sci. 31, 277-283 (2014). https://doi.org/10.5140/JASS.2014.31.3.277

Jung J, Oh S, Yi Y, Evenson P, Pyle R, et al., Installation of neutron monitor at the Jang Bogo station in Antarctica, J. Astron. Space Sci. 33, 345-348 (2016). https://doi.org/10.5140/JASS.2016.33.4.345

Kim EJ, Sohn JD, Yi Y, Ogino T, Lee JH, et al., Martian bow shock and magnetic pile-up barrier formation due to the exosphere ion mass-loading, J. Astron. Space Sci. 28, 17-26

(2011). https://doi.org/10.5140/JASS.2011.28.1.017
Kim SY, Yi Y, Hong IS, Sohn JD, Solar insolation effect on the local distribution of lunar hydroxyl, J. Astron. Space Sci. 35, 47-54 (2018). https://doi.org/10.5140/JASS.2017.35.1.47
Lee JJ, Parks GK, Min K, Kim H, Park J, et al., Energy spectra of ~170–360 keV electron microbursts measured by the Korean STSAT-1, Geophys. Res. Lett. 32, L13106 (2005). https://doi.org/10.1029/2005GL022996
Lee JJ, Parks GK, Min K, McCarthy MP, Lee ES, et al., Relativistic electron dropouts by pitch angle scattering in the geomagnetic tail, Ann. Geophys. 24, 3151-3159 (2006). https://doi.org/10.5194/angeo-24-3151-2006
Moon BH, Jeong DG, Oh S, Sohn, JD, Variation in solar limb darkening coefficient estimated from solar images taken by SOHO and SDO, J. Astron. Space Sci. 34, 99-103 (2017). https://doi.org/10.5140/JASS.2017.34.2.99
Nakamura R, Isowa M, Kamide Y, Baker DN, Blake JB, et al., SAMPEX observations of precipitation bursts in the outer radiation belt, J. Geophys. Res. 105, 15875-15885 (2000). https://doi.org/10.1029/2000JA900018
Park KC, Lee JW, Yi Y, Lee JJ, Sohn JD, Characteristics of solar wind density depletions during solar cycles 23 and 24, J. Astron. Space Sci. 34, 105-110 (2017). https://doi.org/10.5140/JASS.2017.34.2.105.
Parks GK, Microburst precipitation phenomena, J. Geomagn. Geoelectr. 30, 327-341 (1978). https://doi.org/10.5636/jgg.30.327
Shin GH, Chae JS, Lee SH, Min KW, Sohn JD, et al., Operational concept of the NEXTSat-1 for science mission and space core technology verification, J. Astron. Space Sci. 31, 67-72 (2014a). https://doi.org/10.5140/JASS.2014.31.1.67
Shin GH, Chae JS, Min KW, Sohn JD, Jeong WS, et al., Communications link design and analysis of the NEXTSat-1 for SoH file and mission data using CAN bus, UART and SerDesLVDS, J. Astron. Space Sci. 31, 235-240 (2014b). https://doi.org/10.5140/JASS.2014.31.3.235
Sohn JD, Oh SY, Yi Y, Min KW, Lee DY, et al., A design of solar proton telescope for next generatioin small satellite, J. Astron. Space Sci. 29, 343-349 (2012). https://doi.org/10.5140/JASS.2012.29.4.343
Sohn JD, Lee JJ, Min KW, Lee JC, Lee SU, et al., HEPD on NEXTSat-1: a high energy particle detector for measurements of precipitating radiation belt electrons, J. Korean Phys. Soc. 72, 1086-1093 (2018). https://doi.org/10.3938/jkps.72.1086
Sullivan JD, Geometrical factor and directional response of single and multi-element particle telescope, Nucl. Instrum. Method. 95, 5-11 (1971). https://doi.org/10.1016/0029-554X(71)90033-4